Laboratory test of snow wetness influence on electrical conductivity measured with ground penetrating radar

Nils Granlund, Angela Lundberg, James Feiccabrino and David Gustafsson

ABSTRACT

Ground penetrating radar operated from helicopters or snowmobiles is used to determine snow water equivalent (SWE) for annual snowpacks from radar wave two-way travel time. However, presence of liquid water in a snowpack is known to decrease the radar wave velocity, which for a typical snowpack with 5% (by volume) liquid water can lead to an overestimation of SWE by about 20%. It would therefore be beneficial if radar measurements could also be used to determine snow wetness. Our approach is to use radar wave attenuation in the snowpack, which depends on electrical properties of snow (permittivity and conductivity) which in turn depend on snow wetness. The relationship between radar wave attenuation and these electrical properties can be derived theoretically, while the relationship between electrical permittivity and snow wetness follows a known empirical formula, which also includes snow density. Snow wetness can therefore be determined from radar wave attenuation if the relationship between electrical conductivity and snow wetness is also known. In a laboratory test, three sets of measurements were made on initially dry 1 m thick snowpacks. Snow wetness was controlled by stepwise addition of water between radar measurements, and a linear relationship between electrical conductivity and snow wetness was established.

Key words | electrical conductivity, ground penetrating radar, radar wave attenuation, snow, snow water equivalent, snow wetness

Nils Granlund (corresponding author)
Angela Lundberg
James Feiccabrino
Applied Geology, Luleå University of Technology,
97187 Luleå,
Sweden
Tel.: +46 920 491384
Fax: +46 920 491399
E-mail: *nils.granlund@ltu.se*

David Gustafsson
The Royal Institute of Technology (KTH),
Land and Water Resources Engineering,
Stockholm,
Sweden

NOMENCLATURE

A	Resulting wave amplitude
A_0	Effective source amplitude
D_R	Receiver antenna directivity
D_S	Source antenna directivity
G	Geometrical spreading
R	Reflection coefficient
S	Area of a wavefront sector
T	Transmission coefficient
c	Speed of light in vacuum
d	Radar wave trip length
h	Cone frustum height
n	Number of approximation steps
r	Cone frustum radius
t	Radar wave travel time
α	Attenuation (due to energy transformation into heat)
ε	Electrical permittivity
ε_0	Electrical permittivity of free space
ε_r	Relative electrical permittivity
φ	Angle used to define a wavefront sector
θ	Content by volume
μ	Magnetic permeability
μ_0	Magnetic permeability of free space
μ_r	Relative magnetic permeability
σ	Electrical conductivity
ω	Angular velocity of a radar wave

doi: 10.2166/nh.2009.040

INTRODUCTION

Accurate estimates of snow water equivalent (SWE) over large areas are important for the Scandinavian hydropower industry, since good predictions of spring floods (obtained from SWE estimates) allow a more efficient energy production. SWE measurements are also employed by hydrologists in the studies of movement, distribution and quality of water. Moreover, they are useful for climate change research and for the study of the polar ice caps and glaciers.

SWE can be estimated from manually measured snow depth and density. Such measurements are conducted at snow courses, which have to be chosen carefully to represent the area in a satisfying way. Unfortunately, this method is both time-consuming and labour-intensive, with target areas (such as reservoir catchment areas or polar ices) often characterized by poor communications and rough weather conditions.

Measuring SWE with ground penetrating radar (GPR) is an alternative to manual measurements. This method is based on analysis of the two-way travel time of radar wave propagation through a snowpack. The radar can be operated from a helicopter or a snowmobile, which allows covering large areas much faster and cheaper than using traditional manual measurements.

In Sweden, Ulriksen (1982) was the first to conduct research on the use of ground penetrating radar for SWE measurements. Radar operating from a helicopter was first used in 1986 (see Ulriksen (1989) for a good summary of Swedish radar projects for the period 1982–1989). Both ground-based GPR and airborne GPR have been used to measure snow depth and/or SWE, producing similar results (the latter has a tendency to underestimate snow cover depth) (Marchand *et al.* 2003). GPR has also been used to measure snow accumulation rates and SWE in glaciers, with a focus on spatial and temporal variation (Richardson 2001; Pälli 2003; Maurer 2006).

When SWE is measured using ground penetrating radar, it is typically assumed to depend linearly on the radar wave two-way travel time, with coefficients calibrated against manual measurements of SWE. Calibrated SWE measurements with radar have been shown to exhibit a close correspondence to control manual measurements, at least for dry snow with normal density (Andersen *et al.* 1987; Sand & Bruland 1998). However, different coefficients have to be used for different values of snow density (Lundberg *et al.* 2000). Snow density is either measured manually at selected locations (and assumed to be roughly constant throughout the area of interest) (Sand & Bruland 1998), or it is taken to be linearly dependent on snowpack depth (Lundberg *et al.* 2006). It is also possible to determine average snow density for dry snow from radar wave propagation velocity (e.g. with the common mid-point method) using an established empirical relationship between radar wave velocity and snow density. Another solution used in the study of snow accumulation rates and SWE in glaciers is so-called dielectric profiling, where a nonlinear relationship between snow depth and snow density/electrical permittivity/radar wave propagation velocity is established separately for each snow layer using manual measurements at snow pits (Richardson 2001).

However, if the snow is wet, taking into account snow density alone does not produce accurate SWE estimates. For example, it is known that for a snowpack with density around 300 kg/m^3 and 5% (by volume) liquid water SWE is overestimated by approximately 20% (Lundberg & Thunehed 2000). Introduction of liquid water into the snowpack results in a three-phase system (ice, water and air), where SWE cannot be determined from the radar wave two-way travel time unless liquid water content has been determined, even if wave propagation velocity is known. In this case snow density, necessary for the calculation of SWE, has to be estimated from electrical permittivity/radar wave propagation velocity using one of the known empirical formulae for mixtures, all of which contain liquid water content as one of its components (Frolov & Macheret 1999; Sihvola 1999; Lundberg & Thunehed 2000).

It would therefore be beneficial to be able to determine liquid water content using ground penetrating radar and avoid manual measurements. This can be done, for example, by using the frequency shift method to estimate complex electrical permittivity which, with the real part of electrical permittivity determined using the common mid-point method, gives us liquid water content (Bradford & Harper 2006). Our approach, on the other hand, relies on estimating liquid water content in snow from effective electrical

conductivity, which can be obtained from radar wave attenuation, two-way travel time and propagation velocity.

With amplitudes readily available from GPR data, either the effective source amplitude or a reference measurement of amplitude is needed to determine attenuation; the question of determining the reflection coefficient of the snow/ground interface also has to be addressed. When radar wave attenuation has been determined, effective electrical conductivity can be calculated using a formula derived from Maxwell's equations. Then it only remains to establish the relationship between snow wetness and electrical conductivity in order to be able to estimate liquid water content from radar data.

The overall aim of this work is to experimentally establish the relationship between liquid water content (by volume) and effective electrical conductivity of snow, which should lead to an improved accuracy of SWE estimates with ground penetrating radar.

THEORY

In typical GPR applications, the resulting amplitude A depends on effective source amplitude A_0, source and receiver antenna directivity D_S and D_R, geometrical spreading G, reflection coefficient of the target R, attenuation due to energy transformation into heat α (m^{-1}), and trip length d (m). If a radar wave passes several layers with different electromagnetic properties, attenuation and trip length have to be considered separately for each layer and the resulting amplitude also depends on transmission coefficients T_j. When radar waves only travel in one direction without reflection from a target, as is the case in our experiments, there is no reflection term in the formula for resulting amplitude:

$$A = \frac{A_0 D_S D_R}{G} \prod_j T_j e^{-\alpha_j d_j} \tag{1}$$

Let us now consider this equation in detail.

Attenuation

Attenuation in a medium is caused by transformation of a part of electromagnetic energy into heat. For each layer, attenuation α can be derived from Maxwell's equations:

$$\alpha = \omega\sqrt{\frac{\mu\varepsilon}{2}}\left(\sqrt{1+\left(\frac{\sigma}{\omega\varepsilon}\right)^2}-1\right)^{1/2} \approx \frac{\sigma}{2}\sqrt{\frac{\mu}{\varepsilon}} \tag{2}$$

where ω is angular velocity (rad/s), σ is electrical conductivity (S/m), μ is magnetic permeability (Vs/Am) and ε is electrical permittivity (As/Vm) of the medium (Jordan & Balmain 1968). The approximation found in Equation (2) is valid for $\sigma << \omega\epsilon$, which is typical for GPR applications (Annan 2003). Here $\varepsilon = \varepsilon_0 \cdot \varepsilon_r$ and $\mu = \mu_0 \cdot \mu_r$, where ε_r and μ_r are relative values of electrical permittivity and magnetic permeability and the constants ε_0 (As/Vm) and μ_0 (Vs/Am) represent electrical permittivity and magnetic permeability of free space, respectively.

When Equation (2) is used to describe radar wave propagation in a layer where electrical properties vary between different points, such as snow, *effective* electrical conductivity and permittivity have to be considered (Kärkkäinen *et al.* 2001).

Effective relative permittivity of snow can be estimated using an empirical formula for mixtures:

$$(\varepsilon_{r\_\mathrm{snow}})^{1/q} = \theta_{\mathrm{ice}} \cdot (\varepsilon_{r\_\mathrm{ice}})^{1/q} + \theta_{\mathrm{water}} \cdot (\varepsilon_{r\_\mathrm{water}})^{1/q} + \theta_{\mathrm{air}} \cdot (\varepsilon_{r\_\mathrm{air}})^{1/q} \tag{3}$$

where θ is content by volume and q is usually taken to be equal to 3 (Looyenga's formula) or 2 (Birchak's formula) (Frolov & Macheret 1999; Sihvola 1999).

Alternatively, effective relative permittivity can be determined from radar wave travel time t_{snow} (s) and trip length d_{snow} (m):

$$\varepsilon_{r\_\mathrm{snow}} = \frac{c^2 \cdot t_{\mathrm{snow}}^2}{d_{\mathrm{snow}}^2} \tag{4}$$

where c is the speed of light in vacuum (m/s).

Effective source amplitude

Considering Equation (1), we notice that to determine attenuation it is necessary to know effective source amplitude A_0. In the absence of such measurements, it is possible to use amplitude of a reference measurement taken through a medium with well-known electromagnetic

properties: in our case, air. As electrical conductivity of air is equal to zero, the amplitude of a radar wave travelling through air is given by:

$$A_{\text{air}} = \frac{A_0 D_{S\_\text{air}} D_{R\_\text{air}}}{G_{\text{air}}} \tag{5}$$

By positioning the receiver with respect to the source identically in both actual measurement and reference measurements, and ensuring that radar waves follow the same path in both cases (which is achieved by maintaining a 90° angle between the direct line connecting the source and the receiver and all the interfaces between layers, such as the air/snow interface), we obtain $D_{S\_\text{air}} = D_S$ and $D_{R\_\text{air}} = D_R$. Equation (5) yields:

$$A_0 = \frac{A_{\text{air}} G_{\text{air}}}{D_S D_R} \tag{6}$$

Geometrical spreading

Let us first consider a simple model of geometrical spreading where energy is spread equally in all directions from a point source. If radar waves travel in a single homogeneous medium, the wavefront has a spherical shape. However, if radar waves travel through layers with different propagation velocity, the wavefront is no longer spherical as bending occurs at layer interfaces with differing refraction angle which depends on the varying incidence angle (Annan 2003) (Figure 1).

Let us now compare geometrical spreading of a radar wave travelling through several layers with different electrical properties to that of a radar wave propagating through air only, with the same relative position of the receiver with respect to the source. Let us consider a certain angle φ (rad) measured from the direct line connecting the source to the receiver. This angle will define a sector of the wavefront containing the receiver (Figure 1).

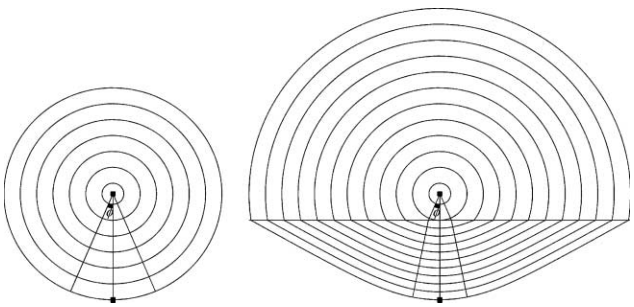

Figure 1 | Cross-section of a 3D wavefront travelling in a single homogeneous medium (left) and from e.g. air to snow (right), with wavefront sectors defined by the same angle φ.

From the principle of conservation of energy, it follows that for a given angle φ the amount of energy spread over the corresponding wavefront sector will be the same in actual and reference measurements. For a sufficiently small angle it is a good enough approximation to assume that the energy is equally spread over the corresponding wavefront sectors, even if our initial assumption that energy is spread equally in all directions from the source is not valid. Geometrical spreading G and G_{air} in Equations (1) and (6), respectively, can therefore be taken equal to a square root of the area of the corresponding wavefront sector, provided that the same angle φ is used for both actual measurements and reference measurements.

For reference measurements through air, the area of the wavefront sector is easily calculated as the area of a sphere segment. For more complicated cases when radar waves travel through two or more layers with different electrical properties, the following approximation can be used.

Let us choose a small angle φ and a number of approximation steps n. Let us then trace (using Snell's law) radar rays from the source at angles $\varphi/n{\cdot}k$, $k = 0,1,2,\ldots,n$ measured from the direct line connecting the source to the receiver. We can then use radar wave propagation velocity in each layer to calculate the points of the wavefront P_k including the receiver P_0. The area of the wavefront sector can then be approximated as a sum of lateral surface areas of right cone frustums, each defined by two adjacent points (Figure 2).

Geometrical spreading for reference measurements through air G_{air} and for actual measurements G can therefore be calculated as follows:

$$G_{\text{air}} = \sqrt{S_{\text{air}}} = \sqrt{2\pi d(1 - \cos\varphi)} \tag{7}$$

$$G = \sqrt{S} = \left(\sum_{k=0}^{n-1} \pi (r_k + r_{k+1}) \sqrt{(r_{k+1} - r_k)^2 + h_k^2} \right)^{1/2} \tag{8}$$

where d is the radar wave trip length from the source to the receiver (m), r_k is the distance from the point of the

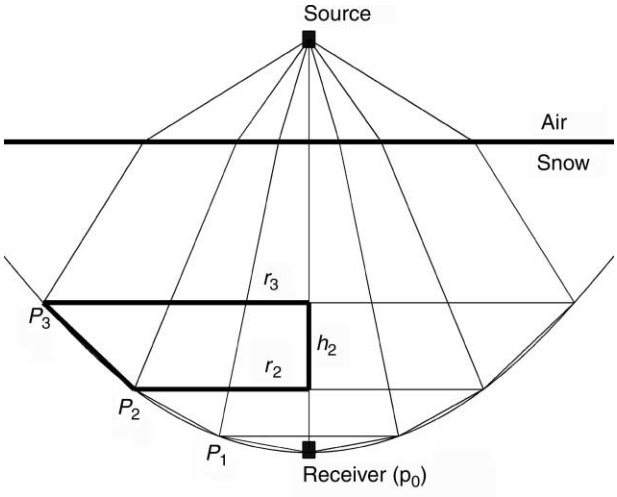

Figure 2 | Approximation of wavefront sector area.

wavefront P_k to the direct line connecting the source and the receiver (m), and h_k is the height of the kth cone frustum (m) (Figure 2).

Transmission coefficients and thin-layer effects

Apart from the above-mentioned attenuation and geometrical spreading, the resulting amplitude of a radar wave depends on scattering at interfaces between layers with different electrical properties. Transmission coefficients for thick interfaces (thick compared to radar wavelength) are given by Fresnel Equations (Tsang 1997). Reflection from thin layers can be substantially smaller (and transmission respectively larger) than specified by Fresnel equations, demonstrated by layers with thickness below 1/10 of radar wavelength not normally reflecting enough energy to be detectable by GPR (Olhoeft 1998) (note that the exact limit of detectability also depends on the contrast in electrical permittivity between adjacent layers).

A special case when the presence of a comparatively thin layer can lead to a considerable change in amplitude can be observed when a direct wave is superimposed with one or several reflected waves 'bouncing' in the thin layer before leaving in the same direction as the direct wave. Depending on layer thickness with respect to radar wavelength and possible phase shifts at interfaces, this radar wave superposition may significantly affect the amplitude at the point of measurement (Annan 2003).

The final formula for radar wave amplitude

Substituting Equations (2) and (6–8) into Equation (1) gives:

$$A = \frac{A_{\text{air}}\sqrt{S_{\text{air}}}}{\sqrt{S}}\prod_j T_j e^{-\alpha_j d_j}, \quad \alpha_j = \frac{\sigma_j}{2}\sqrt{\frac{\mu_0\mu_{r\_j}}{\varepsilon_0\varepsilon_{r\_j}}} \tag{9}$$

Here j traverses all layers encountered by the radar wave, and the areas of the wavefront segments for an actual measurement S and for a reference measurement S_{air} are calculated as described above.

METHOD

A series of three experiments were conducted to establish the relationship between liquid water content and electrical conductivity of snow.

Experiment setup

In each experiment, initially dry snow (initial snow wetness was visibly low when compared to snow wetness observed later in the experiment) was placed in a plywood box with dimensions $0.69 \times 0.70 \times 0.99$ m (width, length and height). In the first two experiments the snow was 'old' with salinity (concentration of total dissolved solids determined from DC conductivity of melted snow at room temperature) 0.0053 g/l and density 285 and 290 kg/m^3, respectively. The third experiment was conducted with fairly recently fallen snow with salinity 0.0028 g/l and density 204 kg/m^3. Prior to the experiments, snow was stored in a climate-controlled room at temperature close to but below 0°C for several days, achieving the temperature of -2 to -4°C at the time of the experiment.

During the experiment, liquid water content of the snow was stepwise increased by adding weighed amounts of water (about 4 and 1 kg in the first experiment and the last two experiments, respectively). The water was sprinkled on the snow surface to achieve an even horizontal distribution of water throughout the snow while keeping the snow surface as plane as possible. The water used in the experiments was tap water chilled to the temperature of 0°C with salinity 0.18 g/l.

After each addition of water, radar measurements were taken through the snow followed by reference measurements through air. Multiple measurements were taken at each step with the resulting radar trace obtained as the average of each measurement set. The equipment used for the experiments was a ground penetrating radar system RAMAC/GPR from Malå Geoscience AB, Malå Sweden, with shielded antennas with 800 MHz centre frequency. A complete description of the equipment and the radar software settings can be found in Granlund (2007).

For actual radar measurements, the antennas were placed near the centre of the upper and lower sides of the box with the receiver precisely under the transmitter. This ensured that radar waves travelled through the snow only in one direction and the direct line connecting the source and the receiver was perpendicular to the snow surface as well as the bottom of the box (Figure 3). The position of the antennas together with the dimensions of the box ensured that the largest cross-section of the first Fresnel volume was inside the snow (Spetzler & Snider 2004; Johnson *et al.* 2005). The antennas were housed in a separate wooden frame (built without any metal parts to avoid interference), which could easily be pulled away from the box for reference measurements through air and which ensured that radar waves followed the same path in both actual and reference measurements (as stipulated in the Theory section).

An inevitable complication was the resulting layering encountered by radar waves during actual measurements; radar waves passed through an air layer above the snow (up to 23 cm thick; the air layer above the snow increased from 20 cm to 23 cm in the first experiment and from 2 cm to 4 cm and to 9 cm in the second and third experiment, respectively), through the snow layer (81, 99 and 99 cm at the beginning of the first, second and third experiments, respectively), through the 2 cm bottom of the box, and finally through a 1 cm air layer below the box. The effect of this layering on the resulting amplitude, including thin-layer effects, is analyzed below.

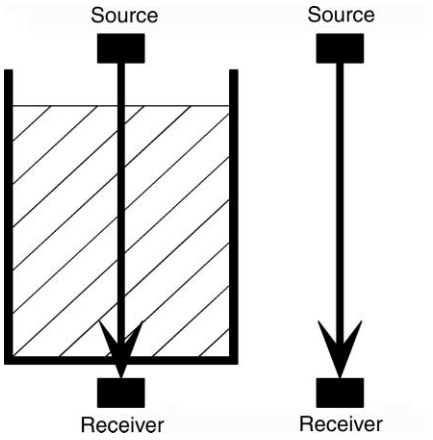

Figure 3 | Experiment setup: radar signals sent through snow (left) and air (right).

Radar data

For each measurement, radar pulse amplitude and one-way travel time had to be determined. Since it was impossible to start recording radar amplitudes at exactly the same time as when the pulse was sent from the transmitter, the pulse *travel time* did not coincide with its recorded *arrival time*. The first clearly identifiable minimum in each radar trace was used to identify the arrival time of the pulse (Figure 4).

With travel time of a reference pulse through air calculated from the distance between the antennas, arrival time of the reference pulse was used to perform time zero correction on the arrival time of the corresponding radar pulse through snow (note that a reference measurement was taken immediately after each actual measurement). Thus the travel time of the pulse was determined; it had to be decreased by the time it took the pulse to travel through the air layers above and below the box, as well as the bottom of the box, to obtain radar pulse one-way travel time in the snow.

Pulse amplitude was defined as the amplitude measured at pulse arrival time, but it had to be corrected for the DC level shift, an increase in the amplitude by a constant value as a result of analogue-to-digital conversion in the receiver. This shift was calculated by taking the average of a number of amplitudes at the beginning of the trace where no transmitted signal was present.

Calculating effective electrical conductivity of snow

After radar pulse amplitudes and one-way travel times had been determined from radar data, effective electrical conductivity was calculated for each value of liquid water content. The formula for electrical conductivity was

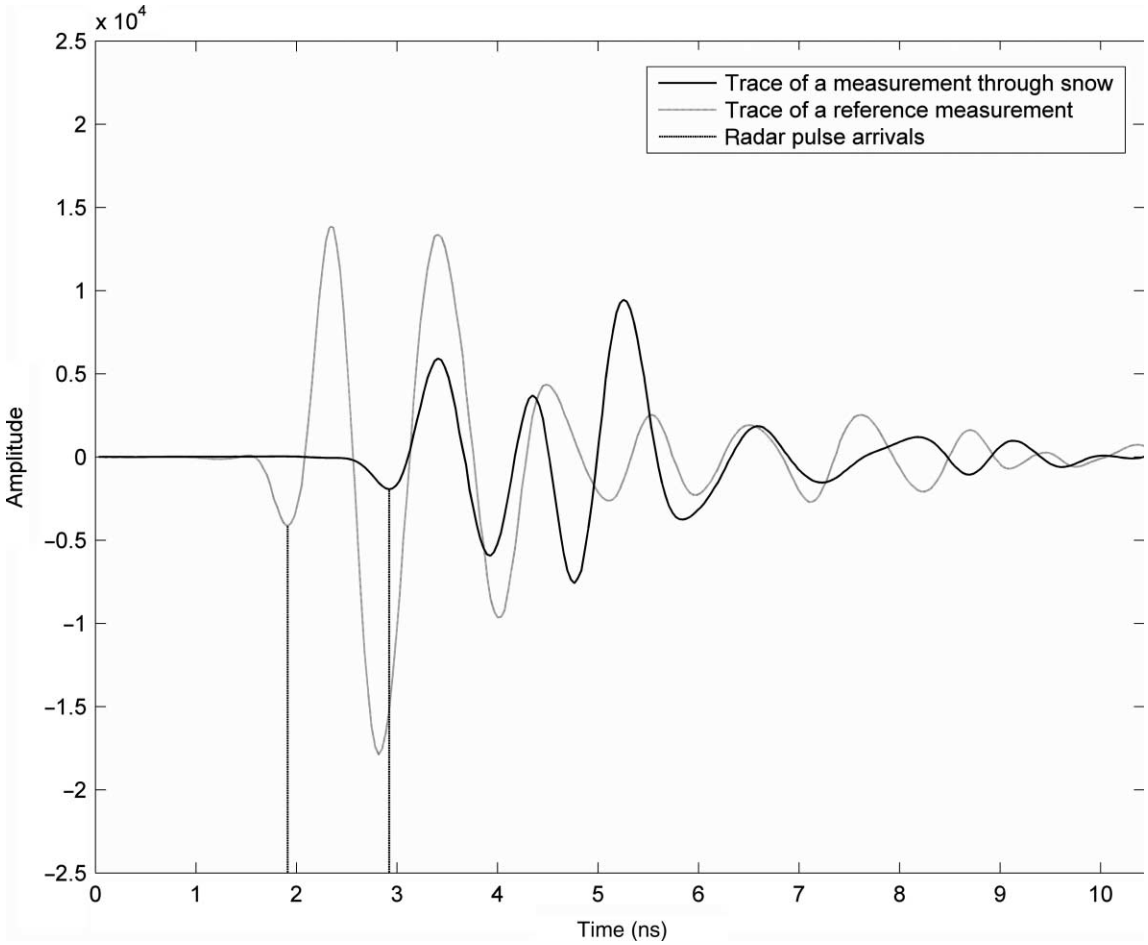

Figure 4 | Radar traces from measurements through snow and air, with radar pulse arrivals.

obtained from Equation (9) with relative magnetic permeability of snow equal to unity ($\mu_{r\_snow} \approx 1$), assuming that attenuation in the air and in the bottom of the box can be neglected:

$$\sigma = -\frac{2}{d_{\text{snow}}}\sqrt{\frac{\varepsilon_0 \varepsilon_{r\_\text{snow}}}{\mu_0}}\ln\left(\frac{A\sqrt{S}}{A_{\text{air}}\sqrt{S_{\text{air}}}\prod_j T_j}\right) \tag{10}$$

Here snow height d_{snow} was assumed to decrease linearly (only the initial and final snow heights were measured). Effective electrical permittivity used in this equation was determined using two methods: estimated using Looyenga's formula (liquid water and ice content by volume were calculated from the mass of added water, the initial mass of snow and the snow volume) (Equation (3) with $q = 3$), and calculated from snow height and radar wave one-way travel time in snow (Equation (4)). The areas of wavefront sectors for reference measurements S_{air} and for actual measurements S were calculated using Equations (7) and (8) with angle $\phi = 0.01°$ and the number of approximation steps $n = 20$.

Three interfaces could cause considerable scattering losses: air/snow, snow/bottom of the box, and bottom of the box/air. Since it is reasonable to assume that layers thinner than 1/10 of the wavelength cause negligible scattering losses at interfaces (see Theory section and Olhoeft 1998), layer thickness was compared with radar wavelength in respective materials. We immediately found that the thickness of the upper air layer varied from 3% to 68% of the wavelength in air while the bottom of the box and the lower air layer constituted about 9% and 3% of the

wavelength in respective media. We could therefore assume that reflection from the second and the third interfaces was insignificant, and it was only necessary to consider scattering losses at the air/snow interface. In these calculations, thin-layer effects of the first and second order in the air above the snow were taken into account.

Analyzing the results

For each value of liquid water content, effective electrical conductivity was calculated:

- with effective electrical permittivity of snow (a) estimated using Looyenga's formula for mixtures, and (b) calculated from radar wave one-way travel time;
- with and without taking into account scattering at the air/snow interface (calculated using Fresnel equations) and thin-layer effects in the air layer above the snow.

In total, four datasets were analyzed: a dataset for each experiment and a fourth dataset containing combined experimental data from all three experiments. On each dataset, linear regression analysis was performed in MATLAB using the least squares method.

RESULTS

The results from experiments 1–3 are presented in Figure 5, with effective electrical conductivity (μS/cm) plotted against liquid water content (vol%). These results were obtained with electrical permittivity calculated from radar wave one-way travel time and without taking into account scattering at the interfaces between layers and thin-layer effects. Equations of linear trend lines for each experiment as well as for combined data from all experiments are presented in Table 1 (first column) together with coefficients of determination.

Other methods of calculating effective electrical conductivity were tested, and it was found that the choice of method of calculating effective electrical permittivity did not significantly influence the results, and neither did taking into account scattering at the air/snow interface together with thin-layer effects in the air layer above the snow. In the latter case, the difference in electrical conductivity was less than 5% in all three experiments. Equations of linear trend lines together with coefficients of determination can be found in Table 1, and the results for the second experiment are presented in Figure 6.

Irrespective of the method used to calculate effective electrical conductivity, the coefficient of determination for the linear trend line for the dataset made up of combined experimental data was very high (97%), and it can serve as the basis of the proposed linear relationship between effective electrical conductivity σ (μS/cm) and liquid water content θ (in volume parts):

$$\sigma = 20 + 3 \times 10^3 \cdot \theta \tag{11}$$

DISCUSSION

Before discussing the obtained results and their projected applicability, let us examine possible sources of error in the obtained experimental data. Several factors besides those taken into account in the equations above could influence radar wave amplitudes and should be considered as possible sources of error.

Firstly, amplitude measurements were affected by multipath interference caused by reflections from the sides of the box and possibly from other objects in the room where the experiments were conducted. The effect of interference was minimized by ensuring that the receiver was not located at an interference maximum or minimum of the direct wave and the waves reflected from the sides of the box. Moreover, any interference should be negligible since the amplitudes were measured at the first clearly defined minimum when the reflected waves had not arrived at the receiver.

Secondly, amplitudes could be affected by planarity of the snow surface. Non-planarity would lead to focusing or dispersion of the radar wavefront and therefore affect the resulting amplitude. To minimize such errors, the snow surface was kept as plane as possible by levelling it at the start of the experiment and by sprinkling water using a watering pot rather than pouring it. Finally, addition of water could lead to formation of waveguides within the snow which could influence the resulting amplitude.

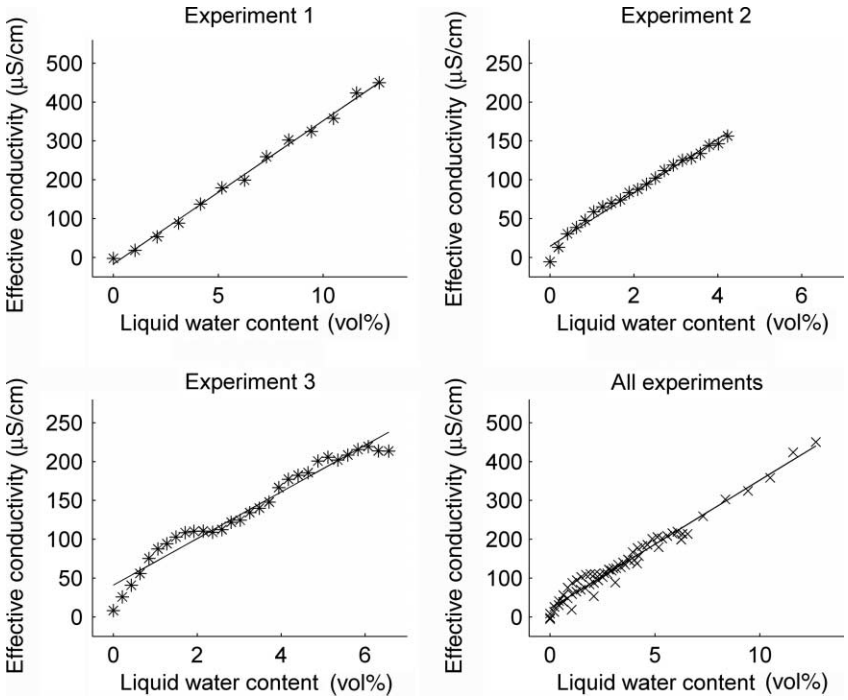

Figure 5 | Data from the experiments with linear trend lines.

Unfortunately, this process would be very hard to prevent or even to detect.

Calculations of liquid water content and ice content relied on two assumptions: that the snow was initially dry and that no substantial state transitions (melting of ice and freezing of water) took place during the experiments. As snow at the start of the experiments was visibly dry compared to its condition later in the course of the experiments, liquid water content, even though not equal to zero, could be assumed to be equal to zero at the start of the experiments. State transitions during the experiments were minimized by keeping the temperature of both snow and water very close to 0°C.

While the average liquid water content in the snow was thus controlled, the question of liquid water content within the volume of snow that affected attenuation the most had to be addressed separately, as it depended on the distribution of water throughout the snow. Sprinkling of water as evenly as possible over the whole snow surface minimized uneven horizontal distribution. Uneven vertical distribution of water, which in the worst case could have caused layering within the snow (with layers having contrasting water

Table 1 | Linear approximation of the relationship between liquid water content θ (in volume parts) and electrical conductivity σ (µS/cm) for different calculation methods

	ε_{r_snow} from one-way travel time		ε_{r_snow} from Looyenga's formula	
	Scattering not included	Scattering included	Scattering not included	Scattering included
Experiment 1	$\sigma = -17 + 3689 \cdot \theta$	$\sigma = -15 + 3559 \cdot \theta$	$\sigma = -7 + 3626 \cdot \theta$	$\sigma = -6 + 3504 \cdot \theta$
	$R^2 = 99.6\%$	$R^2 = 99.6\%$	$R^2 = 99.3\%$	$R^2 = 99.2\%$
Experiment 2	$\sigma = 14 + 3455 \cdot \theta$	$\sigma = 14 + 3400 \cdot \theta$	$\sigma = 15 + 3466 \cdot \theta$	$\sigma = 14 + 3410 \cdot \theta$
	$R^2 = 98.1\%$	$R^2 = 98.0\%$	$R^2 = 97.7\%$	$R^2 = 97.6\%$
Experiment 3	$\sigma = 41 + 3001 \cdot \theta$	$\sigma = 41 + 2924 \cdot \theta$	$\sigma = 43 + 2851 \cdot \theta$	$\sigma = 43 + 2787 \cdot \theta$
	$R^2 = 95.7\%$	$R^2 = 95.4\%$	$R^2 = 94.4\%$	$R^2 = 94.0\%$
Experiments 1–3	$\sigma = 22 + 3303 \cdot \theta$	$\sigma = 23 + 3194 \cdot \theta$	$\sigma = 22 + 3286 \cdot \theta$	$\sigma = 23 + 3180 \cdot \theta$
combined	$R^2 = 97.0\%$	$R^2 = 96.8\%$	$R^2 = 97.2\%$	$R^2 = 97.0\%$

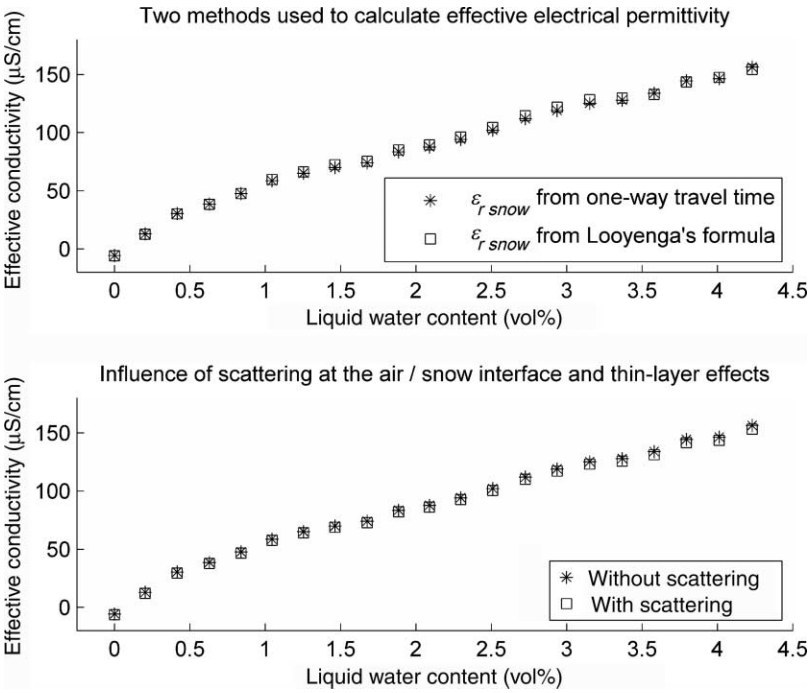

Figure 6 | Variations in electrical conductivity due to different calculation methods (Experiment 2).

content and therefore electrical properties), could be assumed to only have a limited affect on the results since the radar waves travelled the whole height of the snowpack. (Note that a better accuracy of the results can be achieved by performing measurements at multiple points of the snow surface. This would require a box with a considerably larger cross-section area to keep the first Fresnel volume around the radar wave propagation path inside the snow.)

Apart from the above-mentioned sources of error in the experiment setup, several approximations used in calculation of effective electrical conductivity should also be discussed here. One of them was the linear approximation of the decrease in snow height (snow sank with addition of water by 3 and 2 cm in the first two experiments with 'old' snow and by 7 cm in the third experiment with fairly recently fallen snow). This approximation was necessary since only the initial and final values of snow height were recorded. As the approximation error was largest in the third experiment, this could account for a somewhat lower coefficient of determination for the linear trend lines (94–96% instead of 98–99% in the first two experiments; see Table 1).

The model used to account for geometrical spreading losses was also an approximation, partly because energy was not spread equally over a segment of the wavefront and partly because the area itself was calculated by an approximation. However, this approximation should be valid for sufficiently small angles φ, and our tests showed that for small φ (even larger than the value of 0.01° used in our calculations) the quote of geometrical spreading in actual measurements to geometrical spreading in reference measurements remained constant as φ decreased towards zero. It has to be noted, however, that the obtained *negative* values of electrical conductivity for dry snow in the first two experiments (see Figures 5 and 6) (even though they are very close to zero) either indicate that the model of geometrical spreading was incomplete or are a manifestation of some measurement errors.

Having completed an examination of possible sources of error in experiment setup and in calculations of effective electrical conductivity, let us now discuss the results of the experiments and their applicability to improving SWE measurements in the field.

It is clear from the results that neither the choice of the method to estimate effective electrical permittivity (using Looyenga's formula or radar wave one-way travel time), nor including scattering losses at the air/snow

interface together with thin-layer effects in the model of geometric spreading, significantly affects the obtained formula for effective electrical conductivity as a function of liquid water content (Equation (11); see Table 1 and Figure 6). On the other hand, the differences between the formulae obtained for different experiments are somewhat larger (Table 1). The observed spread indicates that the proposed method of determining liquid water content from radar wave attenuation via effective electrical conductivity is likely to have an error margin of about 1% of liquid water content by volume, which is still sufficiently precise to considerably improve SWE estimates for wet snow.

It has to be noted that for the proposed method of determining liquid water content from radar wave attenuation to be usable, we need to be able to determine effective source amplitude and reflection coefficient of the snow/-ground interface. Note also that as the salinity of added water was higher than what is normally found in natural snowpacks, further experiments are needed to determine if and how snow salinity affects the established relationship.

CONCLUSION

The experiments produced promising results paving the way for future use of radar wave attenuation to estimate snow wetness. The results strongly suggest a linear relationship between liquid water content (expressed in volume parts) and effective electrical conductivity (μS/cm) $\sigma = 20 + 3 \times 10^3 \cdot \theta$. However, for this result to be applicable in real life, further studies of snow salinity influence on this relationship as well as studies of attenuation due to reflection from the ground should be conducted. Note also that if initial amplitudes of radar waves are not available, reference measurements will be needed to determine radar wave attenuation in snow.

ACKNOWLEDGEMENTS

The research presented in this article was carried out as a part of Swedish Hydropower Centre (SVC). SVC has been established by the Swedish Energy Agency, Elforsk and Svenska Kraftnät together with Luleå University of Technology, the Royal Institute of Technology, Chalmers University of Technology and Uppsala University (http://www.svc.nu).

REFERENCES

Andersen, T., Lundteigen Fossdal, M., Killingtveit, Å. & Sand, K. 1987 The Snow Radar: A New Device for Areal Snow Depth Measurements. *Proceedings of Workshop on Hydropower in Cold Climates*, *Trondheim*, pp. 1–14.

Annan, A. 2003 *Ground Penetrating Radar, Principles & Applications*. Sensor & Software Inc., Mississauga, Canada.

Bradford, J. H. & Harper, J. T. 2006 Measuring Complex Dielectric Permittivity from GPR to Estimate Liquid Water Content in Snow. *SEG International Exposition and 76th Annual Meeting*. **3**: 1590–1594.

Frolov, A. D. & Macheret, Yu. Ya. 1999 On dielectric properties of dry and wet snow. *Hydrol. Proc.* **13**, 1755–1760.

Granlund, N. 2007 *Improving Snow Water Equivalent Estimates with Ground Penetrating Radar–Laboratory Test of Snow Wetness Influence on Electrical Conductivity of Snow*. M.Sc. Thesis, Luleå University of Technology, Sweden: http://epubl.ltu.se/1402-1617/2007/202/

Johnson, T., Routh, P. & Knoll, M. 2005 Fresnel volume georadar attenuation-difference tomography. *Geophys. J. Int.* **162**, 9–24.

Jordan, E. C. & Balmain, K. G. 1968 *Electromagnetic Waves and Radiating Systems*, 2nd edition. Prentice Hall Inc, New Jersey.

Kärkkäinen, K., Sihvola, A. & Nikoskinen, K. 2001 Analysis of a three-dimensional dielectric mixture with finite difference method. *IEEE Trans. Geosci. Remote Sens.* **39**(5), 1013–1018.

Lundberg, A. & Thunehed, H. 2000 Snow wetness influence on impulse radar snow surveys – theoretical and laboratory study. *Nordic Hydrol.* **31**(2), 89–106.

Lundberg, A., Thunehed, H. & Bergström, J. 2000 Impulse radar snow surveys–influence of snow density. *Nordic Hydrol.* **31**(1), 1–14.

Lundberg, A., Richardson-Näslund, C. & Andersson, C. 2006 Snow density variations: consequences for ground-penetrating Radar. *Hydrol. Proc.* **20**, 1483–1495.

Marchand, W. D., Killingtveit, Å., Wilén, P. & Wikström, P. 2003 Comparison of ground-based and airborne snow depth measurements with georadar system, case study. *Nordic Hydrol.* **34**(5), 427–448.

Maurer, J. 2006 *Local-Scale Snow Accumulation Variability on the Greenland Ice Sheet from Ground-Penetrating Radar (GPR)*. M.Sc. Thesis, University of Colorado at Boulder, USA.

Olhoeft, G. R. 1998 Electrical, Magnetic, and Geometric Properties that Determine Ground Penetrating Radar Performance. *Proceedings of GPR'98, 7th International Conference on Ground Penetrating Radar* 177–182.

Pälli, A. 2003 *Polythermal Glacier Studies in Svalbard Determined by Ground-Penetrating Radar*. PhD Thesis, University of Oulu, Finland.

Richardson, C. 2001 *Spatial Distribution of Snow in Antarctica and Other Glacier Studies Using Ground Penetrating Radar*. PhD Thesis, Stockholm University, Sweden.

Sand, K. & Bruland, O. 1998 Application of georadar for snow cover surveying. *Nordic Hydrol.* **29**(4–5), 361–370.

Sihvola, A. 1999 *Electromagnetic Mixing Formulas and Applications*. The Institute of Electrical Engineers, London.

Spetzler, J. & Snider, R. 2004 The fresnel volume and transmitted waves. *Geophysics* **3**(69), 653–663.

Tsang, T. 1997 *Classical Electrodynamics*. World Scientific Publishing Co. Pte. Ltd, Singapore.

Ulriksen, P. 1982 *Application of Impulse Radar to Civil Engineering*. PhD Thesis, Lund University of Technology, Sweden.

Ulriksen, P. 1989 Radar Measurements of Equivalent Water Content in Snow. Measured from Helicopter. *EARseL Workshops and Symp., Helsinki University of Technology, Espoo, Finland, 27 June–1 July. 1989*, p. 6.

First received 12 December 2007; accepted in revised form 17 October 2008